Spectrochimica Acta Part A: Molecular and Biomolecular Spectroscopy 129 (2014) 52–60

Contents lists available at ScienceDirect

Spectrochimica Acta Part A: Molecular and Biomolecular Spectroscopy

journal homepage: www.elsevier.com/locate/saa

UV–Vis spectroscopic study and DFT calculation on the solvent effect of trimethoprim in neat solvents and aqueous mixtures

M.C. Almandoz [a,*], M.I. Sancho [a], P.R. Duchowicz [b], S.E. Blanco [a]

[a] Área de Química Física, Facultad de Química Bioquímica y Farmacia, Instituto Multidisciplinario de Investigaciones Biológicas (IMIBIO-SL) CONICET, Universidad Nacional de San Luis, 5700 San Luis, Argentina

[b] Instituto de Investigaciones Fisicoquímicas Teóricas y Aplicadas INIFTA (UNLP, CCT La Plata-CONICET), Diag. 113 y 64, Sucursal 4, C.C. 16, 1900 La Plata, Argentina

HIGHLIGHTS

- The solvatochromism of trimethoprim (TMP) was studied by UV–Vis spectroscopy.
- Absorption spectra of TMP were recorded in 13 solvents and 3 binary aqueous mixtures.
- The solvent effects in pure and binary systems were interpreted by Kamlet–Taft LSER.
- Specific solute–solvent interactions were considered in TD-DFT calculations.
- Preferential solvation of organic solvent is observed in all analyzed binary mixtures.

GRAPHICAL ABSTRACT

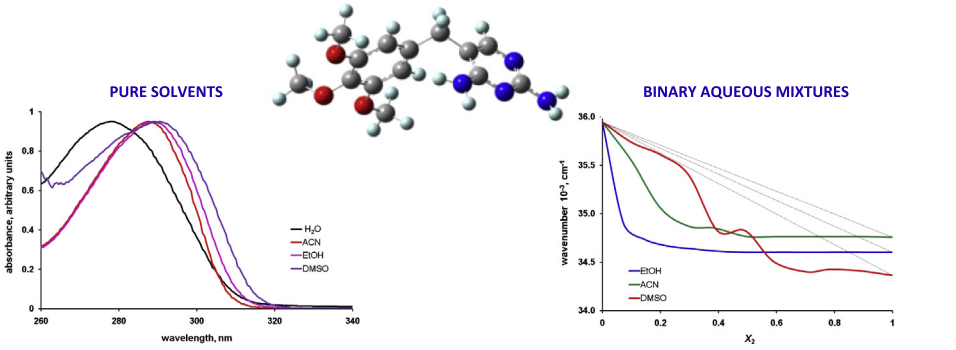

ARTICLE INFO

Article history:
Received 20 December 2013
Received in revised form 21 February 2014
Accepted 25 February 2014
Available online 25 March 2014

Keywords:
Trimethoprim
UV–Vis spectroscopy
Solvatochromism
LSER
Preferential solvation
TD-DFT

ABSTRACT

The solvatochromic behavior of trimethoprim (TMP) was analyzed using UV–Vis spectroscopy and DFT methods in neat and binary aqueous solvent mixtures. The effects of solvent dipolarity/polarizability and solvent–solute hydrogen bonding interactions on the absorption maxima were evaluated by means of the linear solvation energy relationship concept of Kamlet and Taft. This analysis indicated that both interactions play an important role in the position of the absorption maxima in neat solvents. The simulated absorption spectra of TMP and TMP:(solvent)$_n$ complexes in ACN and H_2O using TD-DFT methods were in agreement with the experimental ones. Binary aqueous mixtures containing as co-solvents DMSO, ACN and EtOH were studied. Preferential solvation was detected as a nonideal behavior of the wavenumber curve respective to the analytical mole fraction of co-solvent in all binary systems. TMP molecules were preferentially solvated by the organic solvent over the whole composition range. Index of preferential solvation, as well as the influence of solvent parameters were calculated as a function of solvent composition.

Introduction

Trimethoprim (TMP) [2,4-diamino-5-(3,4,5-trimethoxybenzyl) pyrimidine], is a synthetic antibacterial agent belonging to a group of compounds identified as diaminopyrimidines. This drug prevents the conversion of dihydrofolic acid into tetrahydrofolic acid, resulting in the depletion of the latter and leading to bacterial death. In fact, TMP is the preferred inhibitor of bacterial dihydrofolate reductase in clinical and veterinary use. This is because of its broad spectrum of antibacterial effects, its high degree of selectivity for the bacterial enzyme, and its suitable pharmacodynamic

* Corresponding author. Tel.: +54 266 4520300; fax: +54 266 4430224.
E-mail address: mcalman@unsl.edu.ar (M.C. Almandoz).

http://dx.doi.org/10.1016/j.saa.2014.02.191
1386-1425/

and pharmacokinetic properties. The affinity of TMP for the enzyme in microorganisms is 10,000 times higher than the human enzyme which explains the selective toxicity [1,2]. This compound is active against most common bacterial pathogens and is commonly used in combination with selected sulphonamides. This combination blocks the folic acid metabolism, and thus produces a synergistic antibacterial activity. On the other hand, the use of TMP combined with sulfamethoxazole or sulfametrole for the treatment and prophylaxis of Pneumocystis pneumonia infections in patient with AIDS is of major importance [3]. Used alone its main indication is acute uncomplicated urinary tract infections [4–6]. Therefore, TMP has potential binding sites for metal ions. Several authors have studied the interaction of this ligand with biologically relevant metal ions showing enhanced inhibition than either itself [7–9].

TMP is very slightly soluble in water, slightly soluble in ethanol and acetone and practically insoluble in ether [10]. Due to its low aqueous solubility there are some difficulties in its formulation for instance to intravenous administration. Related to this, the most recent researches are aimed to the use of different surfactants which form inclusion complexes being a strategy to enhance the solubility, stability, and bioavailability of the guest molecules [11,12]. Moreover, ElShaer et al. prepare salts of TMP using anionic amino acids; aspartic and glutamic acid as counter ions in order to improve solubility and dissolution [13].

On the other hand, it is widely known that the behavior of drugs in both neat solvent and solvent mixtures is usually estimated for the purposes of purification, pre-formulation studies, and liquid pharmaceutical dosage forms design [14]. Also, different physicochemical features, such as the rate, progress, and position of the equilibrium of processes as well as the protonation constants are influenced by the solvents in which they are carried out [15–17]. Despite the importance of knowing the behavior of TMP in different solvent systems, no detailed studies are in the literature for this compound, to the best of our knowledge. Therefore, a detailed analysis of this compound solvation, which can influence its solubility and bioavailability, is important and necessary.

In previous reports the solvatochromic characteristics of sulfamethozaxole and flavones were presented [18,19]. As a continuation of this study, in the present work, an experimental and theoretical study on the solvatochromic effects of TMP is performed in single solvents as well as in binary mixture solvents using UV–Vis spectroscopy and DFT methods in order to gain insights on the solute–solvent interactions that this drug presents.

Experimental details

TMP was purchased from Sigma–Aldrich Chemical Co. and was used without further purification. All of the solvents employed were HPLC or spectroscopic grade and were used without further purification: *n*-heptane (*n*-Hp, ⩾99.3%), carbon tetrachloride (CCl_4, ⩾99.9%), chloroform ($CHCl_3$, ⩾99.9%), 1,4-dioxane (Dx, ⩾99.9%), acetonitrile (ACN, ⩾99.8%), N,N-dimethylformamide (DMF, ⩾99.9%), dimethylsulfoxide (DMSO, ⩾99.8%), 1-octanol (1-OcOH, ⩾99.0%), 1-butanol (1-BuOH, ⩾99.9%), 2-propanol (2-PrOH, ⩾99.9%), 1-propanol (1-PrOH, ⩾99.8%) and ethanol (EtOH, ⩾99.9%). They were obtained from Merck KGaA (Germany). Double-distilled water (H_2O) was purified by using a Super Q Millipore System, whose conductivity did not exceed 1.8 μS cm^{-1}.

The concentration of the solutions studied were 1×10^{-4} M. Binary aqueous mixtures of EtOH, ACN and DMSO were prepared from the corresponding solvents by mixing appropriate volumes of each pure solvent in the following ratios: 1:9, 2:8, 3:7, 4:6, 5:5, 6:4, 7:3, 8:2 and 9:1. All the solutions were carefully prepared by weighing on an analytical balance (Acculab, Sartorius Group) with an accuracy of ±0.0001 g and were stabilized at 25.0 ± 0.1 °C for 10 min.

Optical absorption spectra were recorded using a Cary 50-Varian UV–Vis spectrophotometer with thermostatizable quartz cells of 1 cm optical path in the 200–350 nm interval. All spectra were determined at 25.0 ± 0.1 °C and corrected for solvent background by calibrating the instrument to the blank solvent; the experiments were carried out in triplicate and average results were used in the data analysis. The maxima in absorbance for all spectra were obtained with a precision of ±0.5 nm.

Computational details

The initial molecular geometry of TMP was fully optimized with the GAUSSIAN 03 [20] programs package using the hybrid DFT functional B3LYP [21,22] combined with the 6-311++G(d,p) basis set. Initial coordinate of TMP were taken from crystallographic data [23]. The vibrational frequencies were calculated to verify that the minimized structures were true minima. The solvent effect was analyzed on the gas-phase optimized structures by means of the Polarizable Continuum Model with the integral equation formalism (IEF-PCM) [24]. The UAHF radii were employed to build the molecular cavity. Different solute–solvent association complexes were also optimized with the B3LYP/6-311++G(d,p) level of theory. Using the optimized structures in solution of TMP as starting points, vertical excitation energies and the corresponding absorption wavelengths were calculated with the non-equilibrium time-dependant Density Functional Theory (TD-DFT) framework [25], using the same functional and basis set employed in the optimization calculations.

Results and discussion

Solvatochromism of TMP in single solvents

The phenomenon of solvatochromism refers to the effect of solvent, or of a molecule's surrounding (its environment), on some spectroscopic property of that molecule. Most commonly, it concerns to the effect of solvent on the energy at which electromagnetic radiation is absorbed by the probe molecule, it depends on the electronic structure of the solute and solvent molecules, which in turn determines the intermolecular solute–solvent interactions in the ground and the first excited state [26]. The interactions can be classified into: (1) non-specific solute–solvent interaction caused by polarity–polarizability effects and (2) specific solute–solvent interaction such as hydrogen bonding or electron donor acceptor interactions. Spectroscopic techniques are widely used to verify these involved interactions when a solute is added to a solvent. Moreover, absorption spectra depict the character of solvent–solute interaction, which can be predicted from the position, intensity, and shape of the absorption band.

In this work, UV–Vis spectra of TMP were recorded in solvents having different physical–chemical properties. Table 1 summarizes the maximum absorption wavelength (λ_{max}) of TMP in the used solvents, as well as the main solvent parameters: π^* (index of the solvent dipolarity/polarizability), α (measure of the solvent hydrogen-bond donor capacity (HBD)), β (measure of the solvent hydrogen-bond acceptor capacity (HBA)) [27]. Fig. 1 shows as example, the electronic absorption spectra of TMP in seven representative solvents: ACN, DMF, DMSO, $CHCl_3$, 1-PrOH, EtOH and H_2O. In the conversion between wavelength and wavenumber representation of the absorption spectra, the reweighing intensity factor has been taken into account [28]. The UV–Vis absorption spectra of TMP exhibit only one band of maximum absorption between 278.2 and 291.5 nm, depending on the solvent. This λ_{max} value is red

Table 1
Maximum absorption wavelength (λ) and wavenumber ($\bar{\nu}$) of trimetroprim in pure solvents and relevant solvent parameters.

Solvent	λ (nm)	$\bar{\nu}$ (cm^{-1})	ε	α	β	π^*
n-Hp	288.7	34638.0	1.92	0.00	0.00	−0.08
Dx	289.0	34602.1	2.22	0.00	0.37	0.55
Cl_4C	288.3	34686.1	2.24	0.00	0.10	0.28
$CHCl_3$	287.9	34734.3	4.81	0.20	0.10	0.58
1-OcOH	290.2	34459.0	10.30	0.77	0.81	0.40
1-BuOH	289.1	34590.1	17.84	0.84	0.84	0.47
2-PrOH	289.6	34530.4	20.18	0.76	0.84	0.48
1-PrOH	289.5	34542.3	20.80	0.84	0.90	0.52
EtOH	289.0	34602.1	25.30	0.86	0.75	0.54
ACN	287.7	34758.4	36.64	0.19	0.40	0.75
DMF	291.5	34305.3	38.25	0.00	0.69	0.88
DMSO	291.0	34364.3	47.24	0.00	0.76	1.00
H_2O	278.2	35945.4	78.39	1.17	0.47	1.09

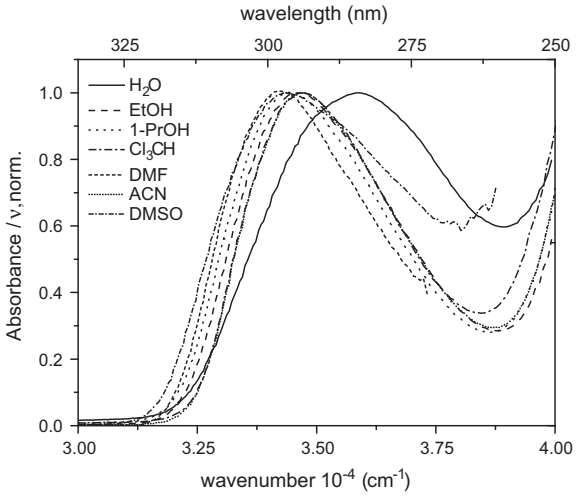

Fig. 1. Normalized absorption spectra of TMP in different solvents.

shifted with respect to water in all the solvents. In aprotic solvents there is a tendency to a red shift when the β parameter increases. In polar protic solvents the λ_{max} shifts to lower wavelengths with increasing solvent polarity. Taking into account, those polar protic solvents with similar α, β and π^* parameters (1-BuOH to 1-PrOH, in Table 1) the λ_{max} are all very close (~289.4 nm). Whereas in this kind of solvents with increasing α values (H_2O > EtOH) and decreasing β values (H_2O < EtOH) hypsochromic shifts are observed (289.0 nm (EtOH) and 278.2 nm (H_2O)).

Fig. 2 shows the optimized molecular structure of TMP calculated at B3LYP/6-311++G(d,p) level of theory. The electronic absorption spectra of this compound were calculated within the TD-DFT framework in two representative solvents: (a) H_2O (polar protic solvent with high α and β values) and (b) ACN (polar aprotic solvent with low α and high β values). The calculated absorption wavelengths ($\lambda_{TD\text{-}DFT}$), oscillator strength (f), molecular orbitals (MOs) involved in the main transitions, and the difference between the experimental and calculated wavelengths ($\Delta\lambda$) are reported in Table 2. From this table it can be observed that the experimental λ_{max} in H_2O is fairly well predicted by the TD-DFT calculations, with a $\Delta\lambda$ of 6.57 nm. Moreover, and taking into account that TMP has the ability to form intermolecular H-bonds with the solvent molecules, the electronic absorption spectra of TMP:$(H_2O)_n$ association complexes were calculated with n = 1 and 2. The results are informed in Table 2 and they indicate that the inclusion of one and two water molecules improves the $\lambda_{TD\text{-}DFT}$ value, reducing the $\Delta\lambda$ value. A comparison between the experimental and calculated spectra of TMP in water is shown in Fig. S1 of the Supplementary Material.

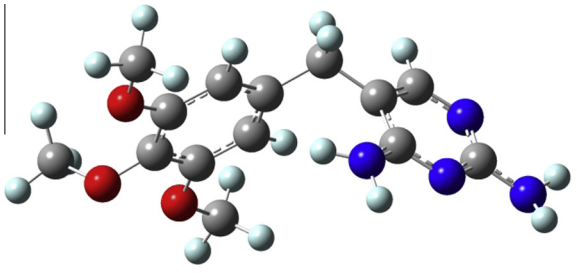

Fig. 2. Calculated structure of minimum energy at B3LYP/6-311++G(d,p) of TMP.

In solution, the changes in the solute geometry would be related with the formation of hydrogen bonds with the solvent molecules, and consequently, with the parts of the molecule more exposed to this interaction. The molecular structures of these TMP complexes are depicted in Fig. 3 and relevant bond lengths and angles are summarized in Table 3. The parameters reported in this table reveal the formation of intermolecular H-bonds of moderate strength between TMP and H_2O molecules [29]. The H_2O molecules considered in the complexes present HBD interactions with the TMP pyrimidinic nitrogens and HBA interactions with the amino groups. Moreover, the bond lengths of HBD interactions are shorter and the bond angles higher than the corresponding of HBA interactions, suggesting that the former are stronger bonds.

Fig. 4 illustrates the shape of MOs involved in the electronic transitions (λ_{max}) of TMP and TMP:$(H_2O)_n$ complexes. The TD-B3LYP results indicate that the main MOs responsible for this transition are HOMO–LUMO with a $\pi\pi^*$ character. The electronic density on the HOMO is delocalized over the whole molecule while in the LUMO the electronic density is localized on the pyrimidin ring, with an important contribution of the nitrogens lone pairs. Taking into account that these lone pairs are involved in the strongest intermolecular H-bond interactions with water molecules, these specific solute–solvent interactions seems to be of great importance in the solvatochromism of TMP in polar protic solvents.

The experimental λ_{max} of TMP in ACN is poorly predicted by TD-B3LYP calculations, compared to the results obtained in H_2O, with a $\Delta\lambda$ value of 17.84 nm. In addition, the calculated spectra of TMP:$(ACN)_n$ (n = 1 and 2) association complexes do not improve the theoretical results. It is important to notice that ACN only presents HBA interactions with the TMP amino groups, since it is an aprotic solvent. The bond lengths of the intermolecular H-bonds between TMP and ACN molecules are between 2.3 and 2.4 Å, indicating that these H-bonds are weaker than the TMP–H_2O intermolecular H-bonds (see Fig. 3 and Table 3). Then, the slight variations in the $\lambda_{TD\text{-}DFT}$ values of TMP and the TMP:$(ACN)_n$ complexes may be attributed to the weak character of these H-bonds [29]. The calculated spectra and the shape of the frontier MOs involve in the electronic transitions of TMP in ACN are illustrated in Figs. S2 and S3 (Supplementary Material), respectively. The HOMO and LUMO of TMP calculated in ACN are coincident with the same MOs calculated in H_2O.

In order to investigate the role of non-specific dipolarity interaction and specific hydrogen bonding ability of solvents, a wide range of solvent parameters such as refractive index (n), dielectric constant (ε) and Kamlet–Taft parameters [30–33], has been extensively used. It is rather difficult to use single macroscopic physical solvent parameters (or functions thereof) in correlating and predicting solvent effects qualitatively and quantitatively. One of the most successful quantitative treatments to analyze this solvent dependence is the linear solvation energy relationships (LSER) [34–37]. The linear relationship between the experimental spectral values and the solvent parameters is as follows:

Table 2
Calculated ($\lambda_{TD\text{-}DFT}$) and experimental (λ_{exp}) wavelengths (in nm) of trimethoprim, and the difference ($\Delta\lambda$) between them. Molecular orbitals (MOs) involved in the main electronic transition. E corresponds to the energy of the transition (in eV) and f is the oscillator strength.

	λ_{exp}	$\lambda_{TD\text{-}DFT}$	IEF–PCM/B3LYP/6-311++G(d,p)			$\Delta\lambda$ (nm)
			f	E	MOs	
TMP[a]	278.2	271.63	0.1487	4.5645	H → L (85%)	6.57
TMP:H_2O		272.90	0.1467	4.5433	H → L (84%)	5.30
TMP:$(H_2O)_2$		273.95	0.1622	4.5258	H → L (84%)	4.25
TMP[b]	287.7	269.86	0.1434	4.5945	H → L (84%)	17.84
TMP:ACN		271.02	0.1479	4.5747	H → L (84%)	16.68
TMP:$(ACN)_2$		270.25	0.1512	4.5877	H → L (84%)	17.45

IEF-PCM/TD-DFT calculation of isolated TMP using:
[a] Water as solvent.
[b] Acetonitrile as solvent.

$$\bar{\nu} = \bar{\nu}_0 + s\pi^* + a\alpha + b\beta \quad (1)$$

where $\bar{\nu}$ is the solute maximum absorption wavenumber, $\bar{\nu}_0$ is the value of this property for the same solute in an hypothetical solvent for which $\pi^* = \alpha = \beta = 0$, and s, a and b are the regression coefficients that measure the relative susceptibility of the solvent dependence of $\bar{\nu}$.

The intermolecular interaction types in TMP solutions have been established on the basis of a multiple linear regression analysis. XLSTAT version 5.1 program has been used to obtain the multiple linear regression coefficients that correspond to peak maximum regression values. Backward stepwise regression was applied to select the significant solvent properties to be influenced in the model. The fitting coefficients obtained from this analysis allowed to estimate the contribution of each type of interactions to the total spectral shifts in the studied solutions.

Applying Eq. (1), the following multiparametric relationship for TMP wavenumber is obtained:

$$\bar{\nu}(\mathrm{cm}^{-1}) = 34,570(95) + 880(112)\alpha - 1284(163)\beta + 728(140)\pi^* \quad (2)$$

$$(n = 13;\ R^2 = 0.911;\ \text{Fisher's } F = 30.58;\ p < 0.000047)$$

The relative contributions of the parameters are: α 30.4%, β −44.4% and π^* 25.2%. The selected variables explain the 91.1% of the variability of $\bar{\nu}$, in different solvents. Fig. 5 displays the plot of the calculated absorption wavenumbers using the above relation as a function of the corresponding experimental values for TMP in the analyzed solvents. As it can be seen from the calculated values achieved with Eq. (2) they are in good agreement with the experimental data, showing a slight deviation when the solvent is $CHCl_3$. The regression coefficients in Eq. (2) are in the order $\beta > \alpha > \pi^*$. This indicates that the hydrogen bonding interactions are significantly responsible for the solvatochromism observed in the absorption spectra, although the influence of solvent polarity cannot be neglected. The signs of β and α coefficients indicate that HBA and HBD solvent characteristics have opposite effects on the position of maximum absorption of TMP.

In order to obtain more detailed information related to solute–solvent interactions, solvents were divided in two groups taking as a classification criterion the α parameter: (i) the first group includes solvents with $\alpha = 0$ and (ii) the second one contains the solvents with $\alpha \neq 0$. The LSER parameters of the backward regression applied to the Eq. (1) for TMP in the first and second groups of solvents with their contributions are shown in Table 4. From this table it could be concluded that in the interaction between TMP and the first group of solvent, the HBA character shows major effect on the maximum absorption wavenumber. The negative sign on the β coefficient indicates that the hydrogen bond formed by the TMP in aprotic solvents may stabilize the excited state more than the ground state, resulting in the observed bathochromic shifts. While when solvents with $\alpha \neq 0$ are analyzed, the spectroscopic characteristics of TMP are determined for both non-specific and specific hydrogen bonding solute–solvent interactions. The contribution of the three parameters (α, β and π^*) must be considered to explain the solvatochromic effect on TMP. Analyzing the signs of these parameters, specific HBA interaction produces a batochromic shift of the TMP absorption band. While dipolar and specific HBD interactions, perform the opposite effect.

Solvatochromism of TMP in binary aqueous mixtures

It is known that the behavior of solutes in mixture of solvents is more complex than in pure solvents and this peculiar performance is due to the alternative for preferential solvation (PS), which takes place when in the vicinity of a solute molecule there is a higher concentration of one solvent than the other, in comparison to the bulk composition. In fact, the solute–solvent and solvent–solvent interactions in mixed solvents can form new solvent entities in the solvation shell of the solute molecules whose properties and their arrangements are distinct and different from those in the neat solvent. In addition, the occurrence of synergistic effects is often observed in studies related to mixed solvents [18,38].

When a binary mixture is considered as an ideal dielectric medium, the maximum absorption wavenumber of the solute follows the lineal additive model according to the next equation [39]

$$\bar{\nu}_{12ideal} = \bar{\nu}_1 X_1 + \bar{\nu}_2 X_2 \quad (3)$$

in which, X_1 and X_2 are the mole fraction of solvents 1 and 2, and $\bar{\nu}_1, \bar{\nu}_2, \bar{\nu}_{12}$ are the values of maximum absorption wavenumber of the TMP in the solvent 1, solvent 2 and the binary mixture, respectively.

If, the experimental values deviate from the linearity, the curvature of plot will indicate that the solute is preferentially solvated by one of the solvents. For that, in order to analyze the interactions observed, the PS approach [40] can be used. This proposal considers the solvent to be distributed between two phases, the bulk and the solvation shell of the solute. It is assumed that the cybotatic region is made up of independent sites that are always occupied. In a non ideal mixture the $\bar{\nu}_{12}$ can be expressed by Eq. (4)

$$\bar{\nu}_{12} = \bar{\nu}_1 X_1^L + \bar{\nu}_2 X_2^L \quad (4)$$

where X_1^L and X_2^L represent the mole fraction of the solvents 1 and 2 in the solvation shell respectively. X_2^L can be calculated from experimental measurements through the following expression:

$$X_2^L = \frac{\bar{\nu}_{12} - \bar{\nu}_1}{\bar{\nu}_2 - \bar{\nu}_1} \quad (5)$$

The index of preferential solvation (δ_{S2}) with respect to the co-solvent [41], can be defined as the difference between X_2^L and X_2.

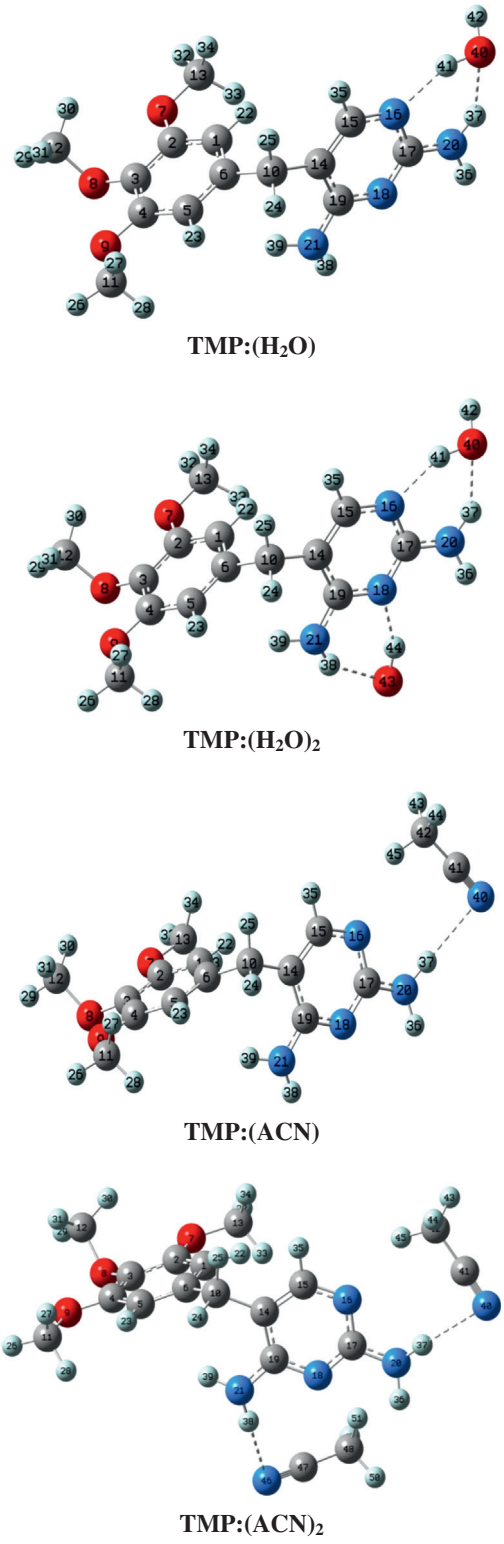

Fig. 3. Molecular structures of the calculated TMP:$(H_2O)_n$ and TMP:$(ACN)_n$ complexes.

$$\delta_{S2} = X_2^L - X_2 \quad (6)$$

A positive value of δ_{S2} indicates a preference for solvent 2 over solvent 1, while a negative value of δ_{S2} signifies vice versa.

Owing to: in several solvents, there is no a substantial difference in the TMP wavelength values (lower than 2 nm) and, the fact that some solvents are not miscible (such as CCl_4–H_2O, 1-OcOH–H_2O), three aqueous mixtures (DMSO, EtOH and ACN) were selected to investigate the effect of solvent composition in the binary systems.

Table 3
Relevant bond lengths (*r*), hydrogen bond length (*d*) and bond angles (*A*) of trimethoprim (TMP) and solute: solvent association complexes measured from B3LYP/6-311++G(d,p) calculations. Bond lengths are reported in Angstrom (Å) and bond angles in degrees (°).

	TMP	TMP:(H_2O)	TMP:(H_2O)$_2$	TMP:(ACN)	TMP:(ACN)$_2$
r $C_{17}N_{20}$	1.370	1.359	1.361	1.361	1.371
r $N_{20}H_{37}$	1.006	1.013	1.014	1.009	1.011
r $C_{19}N_{21}$	1.370	1.368	1.356	1.370	1.360
r $N_{21}H_{38}$	1.009	1.009	1.016	1.009	1.012
d $O_{40}H_{37}$	–	2.109	2.087	–	–
d $N_{16}H_{41}$	–	1.896	1.903	–	–
d $O_{43}H_{38}$	–	–	2.078	–	–
d $N_{18}H_{44}$	–	–	1.917	–	–
A $N_{20}H_{37}O_{40}$	–	142.9	144.2	–	–
A $N_{16}H_{41}O_{40}$	–	154.5	153.3	–	–
A $N_{18}H_{44}O_{43}$	–	–	154.2	–	–
A $N_{21}H_{38}O_{43}$	–	–	145.5	–	–
d $N_{40}H_{37}$	–	–	–	2.392	2.390
d $N_{46}H_{38}$	–	–	–	–	2.314
A $N_{20}H_{37}N_{40}$	–	–	–	178.5	176.6
A $N_{21}H_{38}N_{46}$	–	–	–	–	166.1

Fig. 6 as an example, illustrates the solvatochromic shifts of the absorbance maxima of TMP in H_2O–DMSO binary mixture as a function of the co-solvent mole fraction. In all mixtures, a red shift of the maximum absorption wavelength was observed as the co-solvent mole fraction increases. Also, no important change in the bandwidth and shape with the mixture composition was evidenced. Table 5 summarizes the co-solvent mole fraction in both the bulk and the shell solvation, the wavelength of the maximum absorption and the index of PS for the three binary systems. Plots of $\bar{\nu}_{12}$ versus the bulk mole fraction of the organic solvent (X_2) are shown in Figs. 7–9. The experimental data show that over the whole composition range, TMP is preferentially solvated by the organic solvent, being the H_2O–DMSO behavior slightly different from the others two mixtures.

By looking Fig. 7, two different regions can be distinguished. In the water rich zone ($X_2 \leqslant 0.2$) the solute shows a tendency to an ideal behavior, indicating that the microenvironment (solvation shell) of the solute in this mixture is the same as the bulk composition. While, in DMSO rich region, when the organic solvent concentration is increased, the $\bar{\nu}_{12}$ value diminishes. This pattern begins next to $X_2 = 0.4$ and remains in whole DMSO-rich region. The indexes of PS of TMP in the analyzed interval are listed in Table 5. The positive δ_{S2} values indicate that TMP is preferentially solvated by the organic solvent. The largest obtained value of δ_{S2} in this mixture is 0.320 at $X_2 = 0.590$. The aforementioned PS characteristics of TMP, also would be associated to the non-ideal behavior of this solvent mixture evidenced in different physicochemical properties [42]. In these studies, the largest deviations from ideal mixing at compositions around $X_2 = 0.35$ are observed. The net structure of water is significantly destroyed by the presence of DMSO molecules, thus suggesting the formation of H_2O–DMSO complexes [43]. Hydrogen bonding between DMSO and water molecules is stronger than water–water one. However, no synergistic effect due to the formation of these complexes was observed, indicating that these species do not participate in the preferential solvation of this solute. It is important to highlight that the synergism depends not only on the characteristics of the solvents, but also on the nature of the analyzed solute.

For the others two mixtures (H_2O–ACN and H_2O–EtOH), it can be seen that, at very low organic solvent concentration in the system, important deviations from the ideal behavior occur. This means that there is a prevalence of ACN molecules (Fig. 8) or EtOH

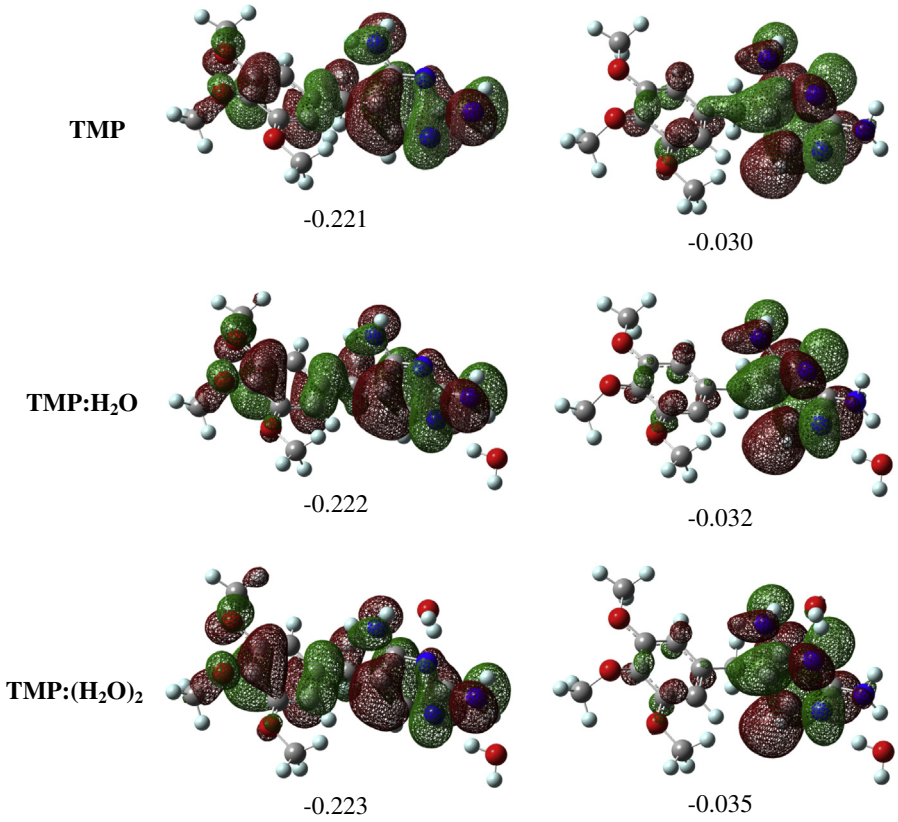

Fig. 4. Molecular orbitals involved in the electronic transitions of TMP and TMP:$(H_2O)_n$ complexes calculated at B3LYP/6-311++G(d,p).

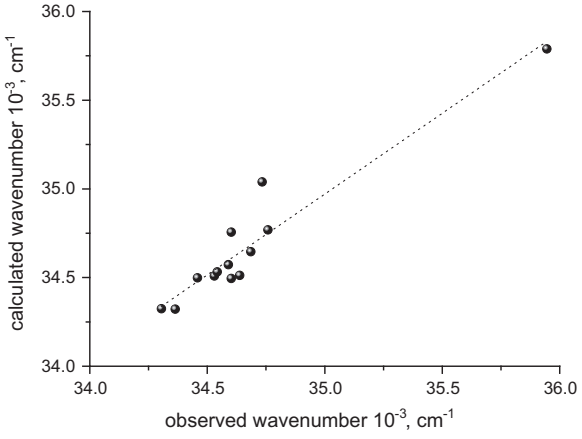

Fig. 5. Calculated absorption wavenumbers using KAT equation as a function of the corresponding experimental values for TMP in the analyzed solvents.

(Fig. 9) in the cybotactic region. During the last years, the H_2O–ACN mixtures have deeply investigated [44]. From these studies, it can be concluded that, two structural phenomena reveal the main interactions between these solvents. The one being the microheterogenity observed at intermediate concentrations and, the other being the possible enhancement of the water structure in very dilute solutions of ACN in water. When TMP is analyzed in this mixture, it is noticed that, in the water-rich zone, the largest PS index is observed ($\delta_{S2} = 0.608$ at $X_2 = 0.300$). At increasing ACN concentrations the values of X_2^L are greater than 0.9 and the δ_{S2} progressively diminishes. This behavior could be explained due to the existence of the microheterogeneity zone, where the ACN molecules self-associate and form microscopic domains, with

Table 4
Contribution and coefficient LSER equation parameters of TMP with the two groups of solvents ($\alpha = 0$ and $\alpha \neq 0$).

Polarity scale	$\alpha = 0$		$\alpha \neq 0$	
	Coefficient	Contribution (%)	Coefficient	Contribution (%)
$\bar{\nu}_0$	34,700 (53)		33,830 (168)	
α	–		743 (152)	26.0
β	−470 (108)	100	−689 (205)	24.2
π^*	–		1421 (211)	49.8
R^2	0.8641		0.9875	

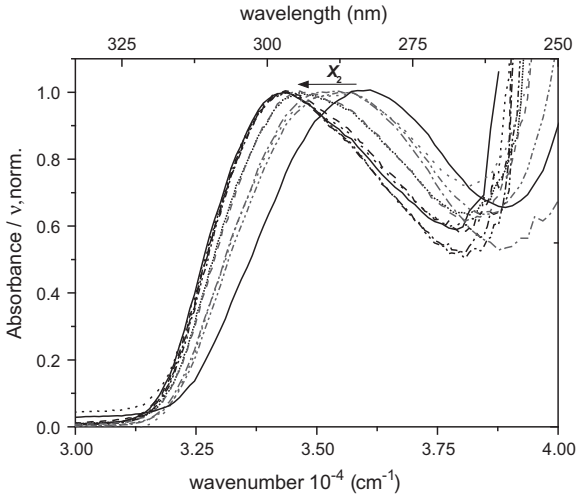

Fig. 6. UV–Vis absorption spectra of TMP in neat solvents (solid lines) and in H_2O–DMSO mixture from $X_2 = 0.103$ to 0.880 (dash lines).

Table 5
Preferential solvation data for trimethoprim in binary aqueous mixtures.

H_2O–DMSO				H_2O–ACN				H_2O–EtOH			
X_2	λ (nm)	X_2^L	δ_{S2}	X_2	λ (nm)	X_2^L	δ_{S2}	X_2	λ (nm)	X_2^L	δ_{S2}
0	278.2			0	278.2			0	278.2		
0.103	279.8	0.133	0.030	0.103	281.3	0.330	0.227	0.073	286.5	0.778	0.705
0.202	280.8	0.213	0.011	0.208	285.3	0.750	0.542	0.144	287.9	0.899	0.755
0.299	282.5	0.346	0.047	0.302	286.8	0.908	0.608	0.228	288.5	0.952	0.724
0.397	287.2	0.710	0.313	0.399	286.9	0.922	0.523	0.318	288.7	0.976	0.658
0.492	287.2	0.710	0.218	0.501	287.7	0.995	0.494	0.404	288.9	0.994	0.590
0.590	289.8	0.910	0.320	0.611	287.7	0.995	0.384	0.511	289.0	0.998	0.488
0.704	290.7	0.978	0.274	0.698	287.7	0.995	0.297	0.588	289.0	0.999	0.411
0.777	290.5	0.963	0.186	0.799	287.7	0.995	0.196	0.709	289.0	0.999	0.290
0.880	290.6	0.970	0.090	0.901	287.7	0.995	0.094	0.903	289.0	0.999	0.096
1	291.0			1	287.7			1	289.0		

X_2: mole fraction of co-solvents (DMSO, ACN or EtOH); λ: maximum absorption wavelength; X_2^L: mole fraction of the solvents 2 (co-solvent) in the solvation shell; δ_{S2}: index of preferential solvation.

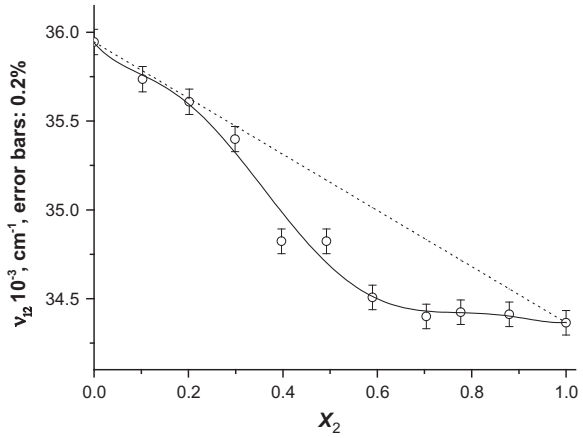

Fig. 7. Plot of $\bar{\nu}_{12}$ for TMP in H_2O–DMSO mixture versus mole fraction (X_2) of co-solvent.

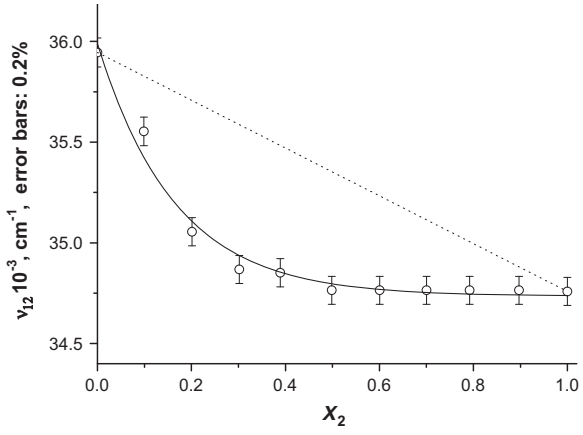

Fig. 8. Plot of $\bar{\nu}_{12}$ for TMP in H_2O–ACN mixture versus mole fraction (X_2) of co-solvent.

water–ACN interactions limited to the interfaces between these areas.

In H_2O–EtOH, the results show that the TMP is preferentially solvated by EtOH in all mole fractions (Fig. 9). It is well known that water makes strong hydrogen-bonded nets in the water-rich region, which are not easily disrupted by the co-solvent [45]. This can explain the strong PS by EtOH in this region since water preferentially interacts with itself rather with the TMP. Therefore, the

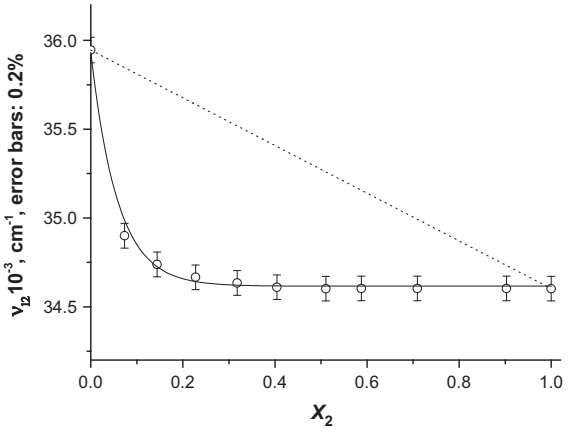

Fig. 9. Plot of $\bar{\nu}_{12}$ for TMP in H_2O–EtOH mixture versus mole fraction (X_2) of co-solvent.

isolated EtOH molecules can interact with the solute, specifically through hydrogen bonding interaction and preferentially enter the solvation sphere of TMP molecules ($\delta_{S2} = 0.755$ at $X_2 = 0.144$). However, in alcoholic rich region, this polar protic solvent gradually disrupts the network of self associated water molecules. Ethanol interacts with water through hydrogen bonding generating water–alcohol aggregated species and therefore the extent of the PS by EtOH diminishes (Table 5).

To obtain a quantitative method to evaluate the interactions of TMP in the binary aqueous mixtures, Eq. (1) was used. The values of the Kamlet–Taft solvatochromic parameters (α, β and π^*) for all water–organic mixtures were taken from the literature [46] that are in some other percentages of the aqueous binary solutions used in this study. So, the reported values of α, β and π^* were separately plotted versus mole fraction of water in order to determine by the fit polynomial, these parameters at the desired mole fraction. The most significant resulting regression equations describing the relationship between $\bar{\nu}_{12}$ and the solvent parameters for TMP are shown below

For H_2O–DMSO

$$\bar{\nu}_{12}(\mathrm{cm}^{-1}) = 32,736(2388) - 3871(932)\beta + 4591(1741)\pi^* \quad (7)$$

($R^2 = 0.9515$; Fisher's $F = 78.45$; $p < 0.000006$)>

For H_2O–ACN

$$\bar{\nu}_{12}(\mathrm{cm}^{-1}) = 33,936(374) - 3016(568)\beta + 3085(250)\pi^* \quad (8)$$

($R^2 = 0.9549$; Fisher's $F = 84.72$; $p < 0.000004$)

For H_2O–EtOH

$$\bar{\nu}_{12}(\mathrm{cm}^{-1}) = 16,444(1863) + 14,166(1203)\alpha + 8054(1127)\beta - 782(173)\pi^* \quad (9)$$

(R^2 = 0.9782; Fisher's F = 104.79; $p < 0.000004$)

Statically, the obtained regression equations demonstrate a very good performance with a squared multiple correlation coefficients (R^2) ranged from 0.9515 to 0.9782. According to the results obtained in the aqueous–aprotic organic solvents systems, such as H_2O–DMSO and H_2O–ACN (Eqs. (7) and (8)) a dual-parametric equation containing β and π^* shows the best fit, thus the solvent effect on the spectral shift of TMP can be satisfactorily explained by a combination of β and π^*. Indeed, the $\bar{\nu}_{12}$ is mainly susceptible to the HBA and polarity solvent properties, with similar contributions but opposite signs. These contributions are $\beta = -45.7\%$ and $\pi^* = 54.3\%$ for H_2O–DMSO and $\beta = -49.4\%$ and $\pi^* = 50.5\%$ for H_2O–ACN. In these mixtures, nonspecific solute solvent association caused by dielectric enrichment in the solvent shell and the specific solute–solvent association such as HBA interactions are present. However, H_2O–EtOH system a multi-parametric equation displays the best fitted model. In the regression analysis of $\bar{\nu}_{12}$ for this mixture (Eq. (9)) although none of the parameters can be neglected, the hydrogen bonding interactions are significantly responsible for the solvatochromism observed in the absorption spectra. The regression coefficients are in the order $\alpha > \beta > \pi^*$ (contributions of 61.6%, 35.0% and −3.4% respectively). In this mixture (protic polar solvents) the solute–solvent hydrogen bonding plays a major role on the solvatochromic properties of TMP giving a shift to lower wavelength in the position of maximum absorption, whereas, in a lesser percentage, the solvent polarity has the opposite effect.

Conclusions

The solvent effect on the electronic absorption spectra of TMP was analyzed in pure solvents and in binary mixtures using UV–Visible spectroscopy and TD-DFT calculations. Linear solvation energy relationships were employed to evaluate the solvatochromic shifts observed in both types of solvents, using the Kamlet and Taft parameters. The solute maximum absorption wavenumbers were correlated with solvent properties by means of single, dual and multiparametric regression analysis. The obtained expressions were useful to explore the nature and extension of solute–solvent interactions in aprotic solvents, polar protic solvent and in binary aqueous mixtures. In neat solvents, the hydrogen bonding interactions are significantly responsible for the TMP solvatochromism, although the influence of solvent polarity cannot be neglected. The electronic transitions of the maximum absorption wavelength, λ_{max}, of TMP and TMP(solvent)$_n$ complexes were studied by means of TD-DFT calculations in two representative solvents (ACN and H_2O). The TD-B3LYP results indicate that the main molecular orbitals responsible for this transition are HOMO–LUMO with a $\pi\pi^*$ character. The electronic density on the HOMO is delocalized over the whole molecule while in the LUMO the electronic density is localized on the pyrimidin ring, with an important contribution of the nitrogens lone pairs. In binary aqueous solvent mixtures (co-solvent: DMSO, ACN and EtOH), the index of preferential solvation was calculated as function of the solvent composition. In all systems, TMP exhibits preferential solvation by the organic solvent in the whole concentration range. LSER results in the aqueous–aprotic organic solvents (H_2O–DMSO and H_2O–ACN) show that a dual-parametric equation containing β and π^* has the best statistical parameters. Thus, $\bar{\nu}_{12}$ is mainly susceptible to the HBA and polarity solvent properties, with similar relative contributions but with opposite signs. However, in a protic polar mixture (H_2O–EtOH), the hydrogen bonding interactions are significantly responsible for the solvatochromism observed in the absorption spectra. The regression coefficients are in the order $\alpha > \beta > \pi^*$.

Acknowledgements

This work was supported by grants from National University of San Luis and by the Consejo Nacional de Ciencia y Tecnología (CONICET) project PIP 11220100100151 (Argentine Republic).

Appendix A. Supplementary material

Supplementary data associated with this article can be found, in the online version, at http://dx.doi.org/10.1016/j.saa.2014.02.191.

References

[1] S. Bhattacharya, P. Sen, A. Ray, Pharmacology, second ed., Elsevier, 2009. pp. 406.
[2] E.P. Quinlivan, J. Mcpartlin, D.G. Weir, J. Scott, FASEB J. 14 (2000) 2519–2524.
[3] L. Huang, A. Cattamanchi, J.L. Davis, S. den Boon, J. Kovacs, S. Meshnick, R.F. Miller, P.D. Walzer, W. Worodria, H. Masur, Proc. Am. Thorac. Soc. 8 (3) (2011) 294–300.
[4] A.V.M. Franco, Best Pract. Res. Clin. Obstet Gynaecol. 19 (2005) 861–873.
[5] K.T. Wisell, G. Kahlmeter, C.G. Giske, J. Antimicrob. Chemother. 62 (2008) 35–40.
[6] L.E. Nicolie, Disease-a-month 49 (2003) 111–128.
[7] P.A. Ajibade, O.G. Idemudia, Bioinorganic Chemistry and Applications, 2013. http://dx.doi.org/10.1155/2013/549549.
[8] B. Simó, L. Perelló, R. Ortiz, A. Castiñeiras, J. Latorre, E. Cantón, J. Inorg. Biochem. 81 (2000) 275–283.
[9] N. Demirezen, D. Tarınc, D. Polat, M. Çeşme, A. Gölcü, M. Tümer, Spectrochim. Acta Part A 94 (2012) 243–255.
[10] A. Xu, T.L. Madden, Analytical Methods for Therapeutic Drug Monitoring and Toxicology, John Wiley & Sons, 2011. p. 465.
[11] S. Göktürk, E. Çalışkan, R.Y. Talman, U. Var, Sci. World J. (2012). Article ID 718791, doi:10.1100/2012/718791.
[12] O.F.L. Macedo, G.R.S. Andrade, L.S. Conegero, L.S. Barreto, N.B. Costa Jr., I.F. Gimenez, L.E. Almeida, D. Kubota, Spectrochim. Acta Part A 86 (2012) 101–106.
[13] A. ElShaer, P. Hanson, T. Worthington, P. Lambert, A.R. Mohammed, Pharmaceutics 4 (2012) 179–196.
[14] J.T. Rubino, in: J. Swarbrick, J.C. Boylan (Eds.), Encyclopedia of Pharmaceutical Technology, vol. 3, Marcel Dekker, New York, 1988.
[15] C. Reichardt, Solvents and Solvent Effects in Organic Chemistry, third ed., Wiley-VCH Verlag GmbH & Co. KGaA, Weinheim, 2003. ISBN: 3-527-30618-8.
[16] S. Sanli, Y. Altun, N. Sanli, G. Alsancak, J.L. Beltran, J. Chem. Eng. Data 54 (2009) 3014–3021.
[17] M. Faraji, A. Farajtabar, F. Gharib, H. Ghasemnejad-Borsa, J. Serb. Chem. Soc 76 (11) (2011) 1455–1463.
[18] M.C. Almandoz, M.I. Sancho, S.E. Blanco, Spectrochim. Acta Part A 118 (2014) 112–119.
[19] M.I. Sancho, M.C. Almandoz, S.E. Blanco, E.A. Castro, Int. J. Mol. Sci. 12 (2011) 8895–8912.
[20] Gaussian 03, Revision B.01, M.J. Frisch, G.W. Trucks, H.B. Schlegel, G.E. Scuseria, M.A. Robb, J.R. Cheeseman, J.A.Jr. Montgomery, T. Vreven, K.N. Kudin, J.C. Burant, J.M. Millam, S.S. Iyengar, J. Tomasi, V. Barone, B. Mennucci, M. Cossi, G. Scalmani, N. Rega, G.A. Petersson, H. Nakatsuji, M Hada, M. Ehara, K. Toyota, R. Fukuda, J. Hasegawa, M. Ishida, T. Nakajima, I. Honda, O. Kitao, H. Nakai, M. Klene, X. Li, J.E. Knox, H.P. Hratchian, J.B. Cross, C. Adamo, J. Jaramillo, R. Gomperts, R.E. Stratmann, O. Yazyev, A.J. Austin, R. Cammi, C. Pomelli, J.W. Ochterski, P.Y. Ayala, K. Morokuma, V.G. Voth, P. Salvador, J.J. Dannenberg, V.G. Zakrzewski, S. Dapprich, A.D. Daniels, M.C. Strain, O. Farkas, D.K. Malick, A.D. Rabuck, K. Raghavachari, J.B. Foresman, J.V. Ortiz, Q. Cui, A.G. Baboul, S. Clifford, J. Cioslowski, B.B. Stefanov, G. Liu, A. Liashenko, P. Piskorz, I. Komaromi, R.L. Martin, D.J. Fox, T. Keith, M.A. Al-Laham, C.Y. Peng, A. Nanayakkara, M.P. Challacombe, M.W. Gill, B. Johnson, W. Chen, M.W. Wong, C. Gonzalez, J.A. Pople. Gaussian Inc., Pittsburgh PA, 2003.
[21] A.D. Becke, Phys. Rev. A 38 (1988) 3098–3100.
[22] C. Lee, W. Yang, R.G. Parr, Phys. Rev. B 37 (1988) 785–789.
[23] T.F. Koetzle, G.J.B. Williams, J. Am. Chem. Soc. 98 (1976) 2074–2078.
[24] E. Cancès, B. Mennucci, J. Tomasi, J. Chem. Phys. 107 (1997) 3032–3041.
[25] R.E. Stratmann, G.E. Scuseria, M.J. Frisch, J. Chem. Phys. 109 (1998) 8218–8224.
[26] P.W. Carr, Microchem. J. 48 (1993) 4–28.
[27] Y. Marcus, Chem. Soc. Rev. 22 (1993) 409–416.
[28] G. Angulo, G. Grampp, A. Rosspeintner, Spectrochim. Acta Part A 65 (2006) 727–731.
[29] G.A. Jeffrey, An Introduction to Hydrogen Bonding, Oxford University Press, Oxford, 1997. 12–16.

[30] M. Józefowicz, J.R. Heldt, J. Heldt, Chem. Phys. 323 (2006) 617–621.
[31] O.A. Adegoke, O.S. Idowu, Spectrochim. Acta Part A 75 (2010) 719–727.
[32] M. Panigrahi, S. Dash, S. Patel, B.K. Mishra, J. Phys. Chem. B 115 (2011) 99–108.
[33] C. Reichardt, Solvents and Solvent Effects in Organic Chemistry, third ed., Wiley-VCH Verlag GmbH & Co., KGaA, Weinheim, 2003.
[34] S.N. Azizi, M.J. Chaichi, M. Yousefi, Spectrochim. Acta Part A 73 (2009) 101–105.
[35] İ. Sıdır, Y. Gülseven Sıdır, H. Berber, E. Taşal, J. Mol. Liq. 178 (2013) 127–136.
[36] N. Tekin, H. Pir, S. Sagdinc, Spectrochim. Acta Part A 98 (2012) 122–131.
[37] S.E. Blanco, E.I. Gasull, F.H. Ferretti, Spectrochim. Acta Part A 59 (2003) 2985–2995.
[38] F.M. Testoni, E.A. Ribeiro, L.A. Giusti, V.G. Machado, Spectrochim. Acta Part A 71 (2009) 1704–1711.
[39] A. Ben-Naim, J. Phys. Chem. 93 (1989) 3809–3813.
[40] L.S. Frankel, C.H. Langford, T.R. Stengle, J. Phys. Chem. 74 (1970) 1376–1381.
[41] P. Chatterjee, S. Bagchi, J. Phys. Chem. 95 (1991) 3311–3314.
[42] N. Engel, K. Atak, K.M. Lange, M. Gotz, M. Soldatov, R. Golnak, E. Suljoti, J. Rubensson, E.F. Aziz, J. Phys. Chem. Lett. 3 (2012) 3697–3701.
[43] B. Kichner, Phys. Rep. 440 (2007) 1–111.
[44] Y. Marcus, J. Phys. Org. Chem. 25 (2012) 1072–1085.
[45] D. Pečar, V. Doleček, Fluid Phase Equilibria 230 (2005) 36–44.
[46] Y. Marcus, J. Chem. Soc., Perkin Trans. 2 (8) (1994) 1751–1758.